Electronic Supplementary Material (ESI) for Physical Chemistry Chemical Physics.

Supporting Information

Enhancing photocatalytic overall water splitting performance on dual-active-sites of the Co-P@MoS_2 catalysts: A DFT study

Jing Ma[a], Xin Wang[a,*], Dongchun Yang[b], Jianhua Fan[a], Xiaoyong Lai[a], Roberts I. Eglitis[c], Yingtao Liu[a,*]

[a] *State Key Laboratory of High-Efficiency Utilization of Coal and Green Chemical Engineering, National Demonstration Center for Experimental Chemistry Education, College of Chemistry and Chemical Engineering, Ningxia University, Yinchuan 750021, China.*

[b] *Institute of Chemistry Chinese Academy of Sciences, 100190 Beijing, PR China*

[c] *Institute of Solid State Physics, University of Latvia, 8 Kengaraga Str., Riga LV1067, Latvia*

[*]Corresponding author.

E-mail address: wangxin@nxu.edu.cn(X., Wang); liuyt@nxu.edu.cn (Y. T., Liu)

Text S1. Nonadiabatic molecular dynamics with time-domain density functional theory

Our calculations employ ab initio nonadiabatic molecular dynamics (NAMD) implemented within time-domain density functional theory (TD-DFT) in Kohn-Sham theory (KS) framework to simulate the photogenerated electron dynamics.

The electron density at time t ($\rho(\mathbf{r}, t)$) is expressed in the Kohn-Sham (KS) formulation as follows:

$$\rho(\mathbf{r}, t) = \sum_{n=1}^{Ne} | \psi_n(\mathbf{r},t) |^2 \quad (1)$$

where n = 1, 2, …, *Ne*, and *Ne* is the number of electrons.

The evolution of the electron density is given by applying the time-domain variational principle to the KS energy as follows:

$$i\hbar\frac{\partial}{\partial t}\psi_n(\mathbf{r},t) = H(\mathbf{r}, \boldsymbol{R}, t)\psi_n(\mathbf{r}, t) \quad (2)$$

where the Hamiltonian ($H(\mathbf{r}, \boldsymbol{R}, t)$) depends on the electron density and its gradient. We expand the time-dependent KS orbitals on the basis of adiabatic KS orbitals, $\phi_k(\boldsymbol{r}; R(r))$, which are the eigenstates of the KS Hamiltonian for the current atomic position, **R**.

The time-dependent KS orbitals are obtained by solving the time-independent KS equation at configuration **R**(t) as follows:

$$\psi_n(\mathbf{r},t) = \sum_k C_k^n(t)\phi_k(r; R(r)) \quad (3)$$

R is obtained from molecular dynamics (MD).

Equations-of-motion for the coefficients are obtained through the combination of

eq 2 and eq 3 as follows:

$$i\hbar\frac{\partial}{\partial t}C_j^n(t) = \sum_k C_k^n(t)(\varepsilon_k\delta_{jk} + d_{jk} \quad (4)$$

where d_{jk} is the nonadiabatic coupling (NAC) between the adiabatic KS orbitals *k*, *j*, and ε_k is the eigenenergy associated with the adiabatic KS orbital *k*. NAC arises from the dependence of the adiabatic orbitals on the nuclear coordinates, **R**, and is computed numerically as the overlap between the adiabatic orbitals k and j in sequential time steps.

Here, ε_k is the energy of the adiabatic KS state and d_{jk} is the NAC between the KS states *j* and *k*. The NAC can be written as:

$$d_{jk} = -i\hbar\langle\phi_j|\nabla_R|\phi_k\rangle \cdot \frac{dR}{dt} = -i\hbar\langle\phi_j\left|\frac{\partial}{\partial t}\right|\phi_k\rangle \quad (5)$$

The many-particle formulation of the above formalism and the implementation are detailed in ref [1].

Simulation details of Hefei-NAMD as follows:

After geometry optimization, the systems are heated to 300 K by repeated velocity rescaling. Then, a 5 ps adiabatic MD trajectory is obtained in the microcanonical ensemble with a 1 fs atomic time step. To simulate the charge-carrier recombination dynamics on a nanosecond time scale, the 5 ps nonadiabatic Hamiltonians are iterated 200 times. The simulation results are based on averaging over 50 random initial configurations and 2000 surface-hopping trajectories sampled for each initial structure.

Text S2 Calculation of formation energy.

The formation energy is concluded by fixing the Co atom and placing the P atom in different positions. For Co@MoS_2, E_{form} is given by the following formula [2]:

$$E_{form} = E_{tot} - E_{MoS_2} - E_{Co} + E_{Mo} \quad (1)$$

where E_{tot} and E_{MoS_2} are the total energy of the pristine MoS_2 with and without Co doped by DFT concluded, respectively. E_{Co} and E_{Mo} are the chemical potentials of the Co and Mo atom, respectively.

The formation energy (E_{form}) for the modification of P in Co@MoS_2 is calculated by using the following formula:

$$E_{form} = E_{tot} - E_{Co@Mos_2} - E_P + E_S \quad (2)$$

where E_{tot} and $E_{Co@MoS_2}$ are the total energy of Co-P@MoS_2 with and without P doped by DFT concluded, respectively. E_P and E_S are the chemical potential of the P atom and S atoms, respectively.

The chemical potential was calculated using the free energies of H_2, H_2S and black phosphorus (1 × 1 × 1) as references. Its calculation formula is as follows [3]:

$$\mu(H) = 1/2G(H_2) \quad (3)$$

$$\mu(S) = G(H_2S) - G(H_2) \quad (4)$$

$$\mu(Mo) = G(MoS_2) - 2\mu(S) \quad (5)$$

$$\mu(P) = 1/4G_{black\ phosphorus} \quad (6)$$

where G (H_2) and G (H_2S) are the energy of the gas molecules. The G (MoS_2) and G (black phosphorus) are the energy of E (MoS_2) and E (black phosphorus) by DFT

concluded, respectively. The energy of species is shown in Table S1.

Table S1. The energy of species in Vacuum.

	H_2	H_2S	P	Mo	Co	H_2O
Energy (eV)	-6.76	-11.24	-4.12	-13.38	-5.20	-14.23

Text S3 Thermal stability

To examine the thermal stability of the Co-P@MoS_2, the ab initio molecular dynamics (AIMD) has been simulated ~~by~~ using Nosé thermostat model [4]. we have considered a 4 × 4×1 supercell to perform the simulation at 300 K, 500 K and 700 K temperatures for 5 picoseconds (ps) with a time step of 1 femtoseconds (fs). To balance the calculation speed and accuracy, relatively sparse 3 × 3 × 1 k-mesh is employed in AIMD simulations for integral sampling.

Text S4 Calculation of the free Gibbs energy change for OER and HER

For OER, the free Gibbs energy change of four steps can be expressed as [5]:

$$\Delta G_1 = G_{OH*} + 1/2G_{H_2} - G_{H_2O} - G* \quad (8)$$

$$\Delta G_2 = G_{O*} + 1/2G_{H_2} - G_{*OH} \quad (9)$$

$$\Delta G_3 = G_{OOH*} + 1/2G_{H_2} - G_{H_2O} - G_{O*} \quad (10)$$

$$\Delta G_4 = G* + 1/2G_{H_2} + G_{O_2} - G_{OOH*} \quad (11)$$

$$\Delta G_5 = G_{H*} - 1/2G_{H_2} + G* \quad (12)$$

where G_* denotes the ~~the~~ free Gibbs energy of the catalyst. The G_{*OH}, G_{*O}, G_{*OOH}, and G_{*H} denote the free Gibbs energy of the oxygenated species adsorbed on the catalyst, respectively.

Table S2. For Co-P@MoS_2, zero-pint energy correction (E_{ZPE}), entropy contribution (TS, T=298.15K), total energy (E) and Gibbs free energy (G) of molecules and adsorbates on the P site.

Species	E_{ZEP} (eV)	-TS	E (eV)	G (eV)
OH*	0.36	-0.09	-353.26	-352.99
O*	0.08	-0.06	-349.42	-349.40
OOH*	0.36	-0.18	-357.53	-357.35
H*	0.23	-0.01	-353.89	-353.67

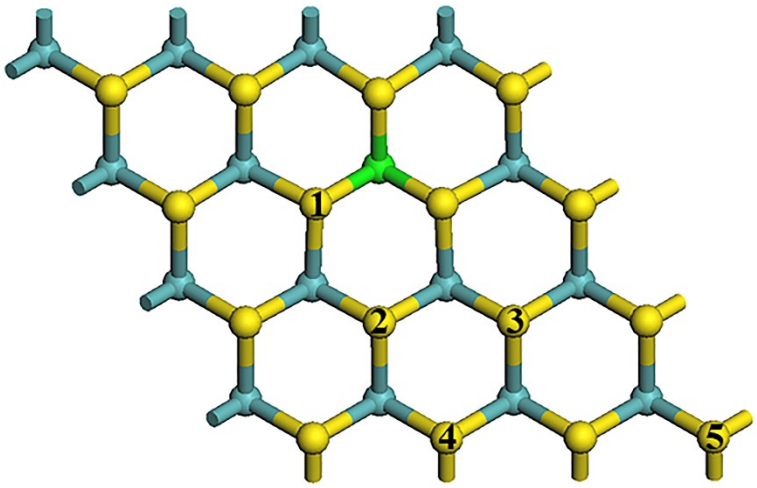

Fig. S1. The geometric structure of the Co-P@MoS_2. The number represents where the P atom is going to replace the S atoms. The blue, yellow and green balls stand for Mo, S and Co atoms, respectively.

Table S3. The value of formation energy was obtained with fixing the Co atom and placing the S atom in different positions.

	P in position 1	P in position 2	P in position 3	P in position 4	P in position 5
The formation energy (eV)	-1.19	-0.72	-0.67	-0.59	-0.53

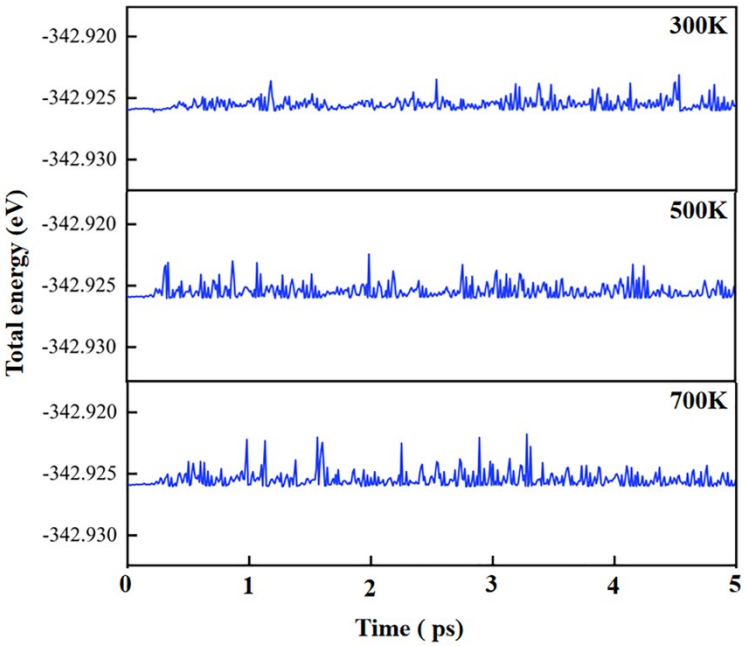

Fig. S2 AIMD simulations of the Co@MoS_2 for 5 ps with a time step of 1 fs at 300 K, 500 K, and 700 K temperatures.

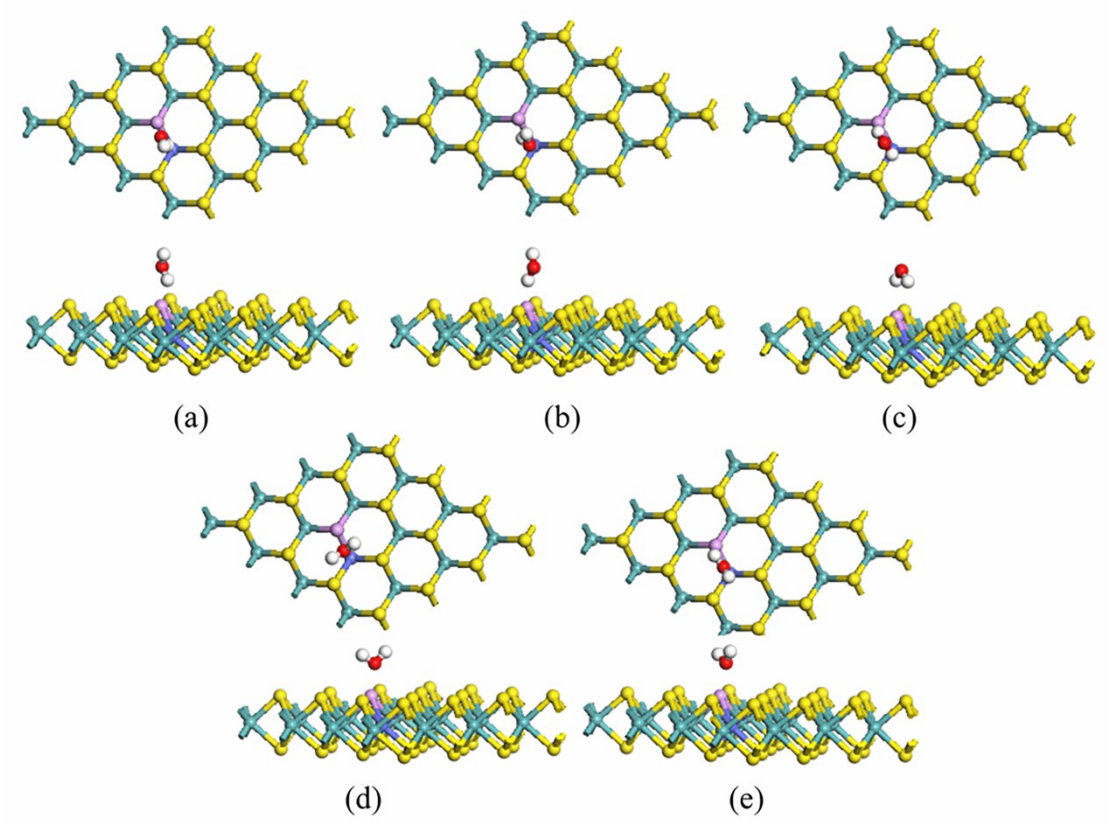

Fig. S3 Top and side views of different orientations of H_2O adsorption on the Co-P@MoS_2 surface

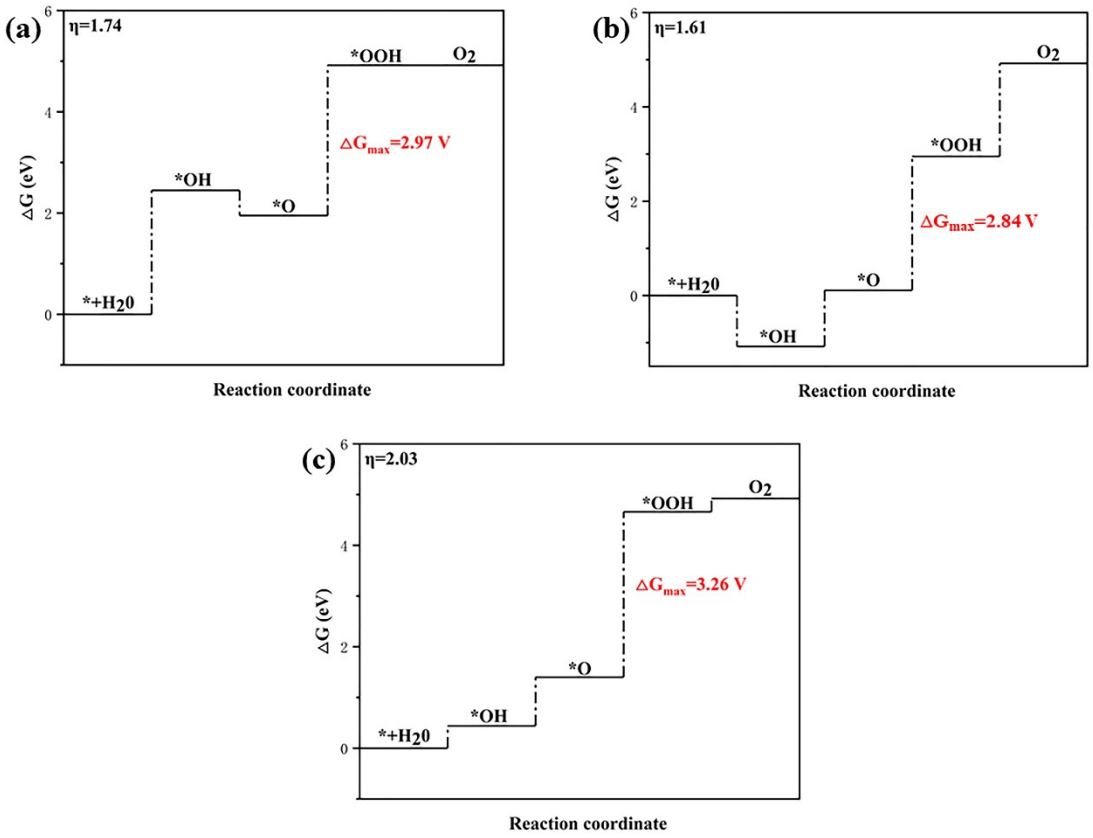

Fig. S4 Elementary reactions and free energy diagrams four electron water oxidation on (a) the pristine MoS_2, (b) P@MoS_2 and (c) the Co@MoS_2, respectively.

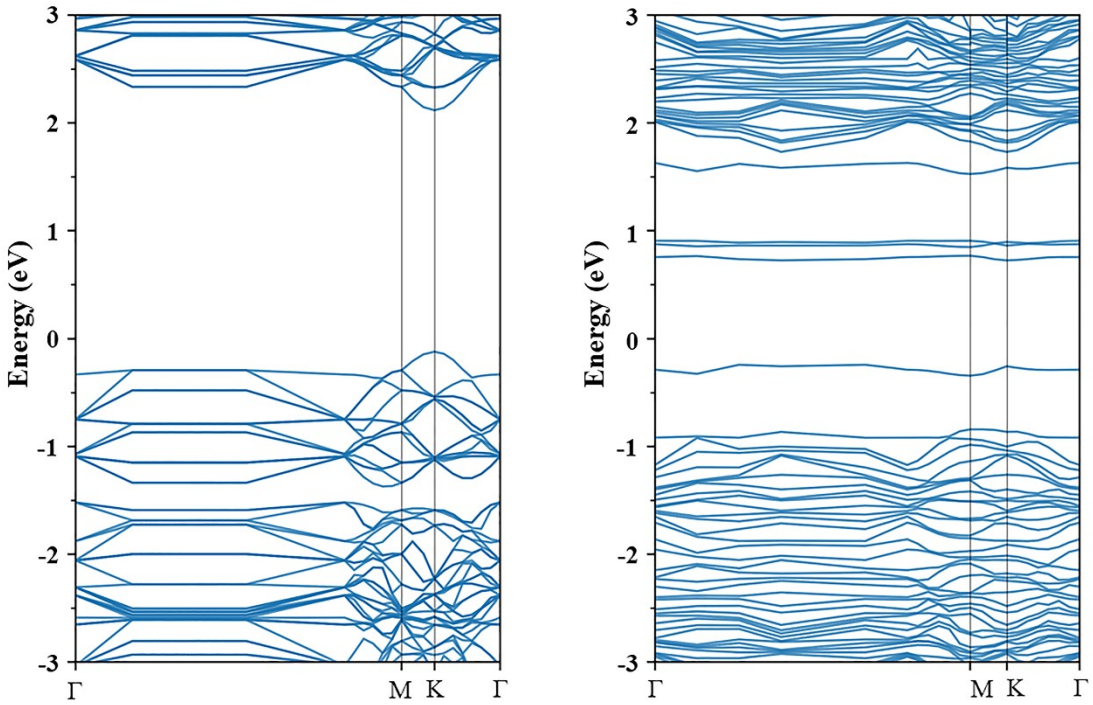

Fig. S5. The band structure of (a) the pristine MoS_2 and (b) the Co-P@MoS_2.

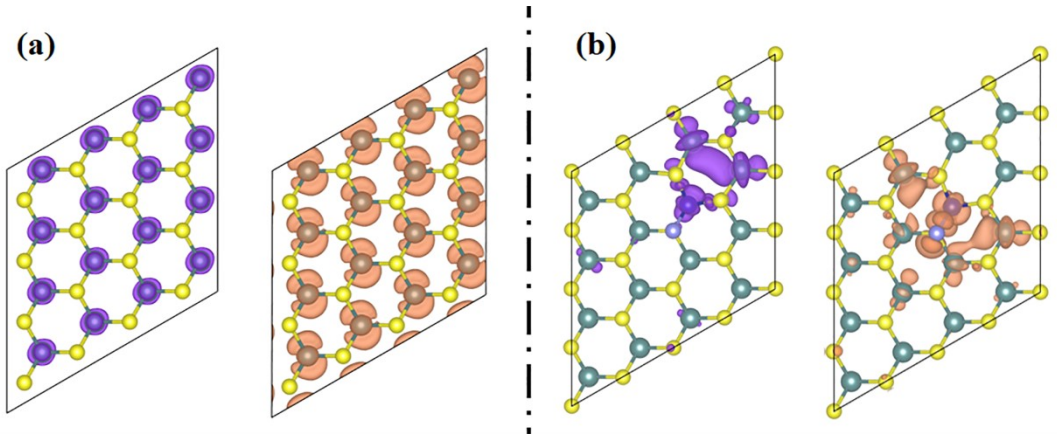

Fig. S6 The HOMO and LUMO of (a) the pristine MoS_2 and (b) the Co-P@MoS_2, with an isosurface of 0.02e/Bohr^3. For the pristine MoS_2, the HOMO and LUMO overlap on all the Mo atoms. For the Co-P@MoS_2, the HOMO and LUMO partially separate at different Mo or doped atoms. The purple and brown regions represent HOMO and LUMO, respectively.

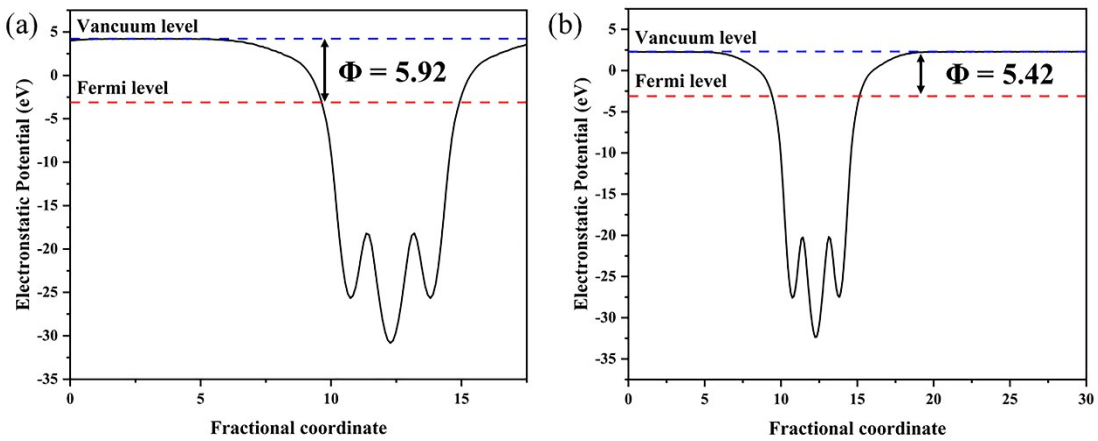

Fig. S7. Work functions of (a) the pristine MoS_2 and (b) the Co-P@MoS_2.

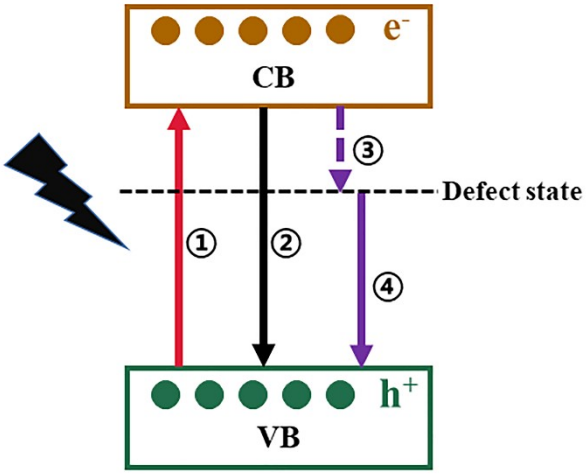

Fig. S8. After illumination, the initial state corresponds to the electron excitation from the valence band (VB) to the conduction band (CB) (process ①). During the relaxation process, electrons in the CB can directly recombine with holes in the VB (process ②). A partial photoexcited electrons can get trapped by the defect state (process ③). Following the releas, electrons can undergo recombination with the VB holes (process ④).

Fig. S8 shows a diagram of the electronic energy levels involved in the charge carrier trapping and relaxation dynamics for the pristine and defective MoS_2 monolayers. After illumination, the initial state corresponds to the electron excitation from the valence band (VB) to the conduction band (CB) (process ①). This process corresponds to the red line in Fig. 7. Before the electrons are excited, the electron population is 1, which means 100 percent. Then, the excited electrons in the CB can recombine with the VB holes through two ways. One way is to directly recombine with holes in the VB (process ②). This process corresponds to the black line in Fig. 7. The other way is that partial photoexcited electrons are first trapped by the defect state and then recombine with the VB holes (processes ③ and ④). This process corresponds to the purple line in Fig. 7.

Notes and References:

1. A. V. Akimov and O. V. Prezhdo, *J Chem Theory Comput*, 2013, **9**, 4959-4972.
2. J. Ge, D. Zhang, Y. Qin, T. Dou, M. Jiang, F. Zhang and X. Lei, *Appl. Catal. B*, 2021, **298**, 120557-120565.
3. Z. Zheng, L. Yu, M. Gao, X. Chen, W. Zhou, C. Ma, L. Wu, J. Zhu, X. Meng, J. Hu, Y. Tu, S. Wu, J. Mao, Z. Tian and D. Deng, *Nat Commun*, 2020, **11**, 3315.
4. S. Nosé, *J Chem Phys*, 1984, **81**, 511-519.
5. M. Qiao, J. Liu, Y. Wang, Y. Li and Z. Chen, *J Am Chem Soc*, 2018, **140**, 12256-12262.